

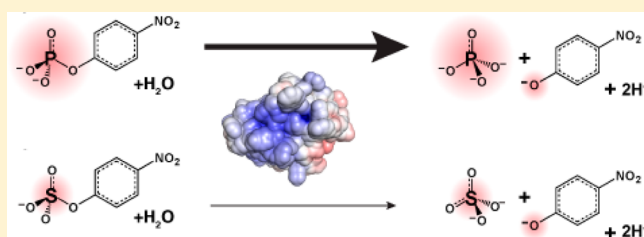
# Probing the Origins of Catalytic Discrimination between Phosphate and Sulfate Monoester Hydrolysis: Comparative Analysis of Alkaline Phosphatase and Protein Tyrosine Phosphatases

Logan D. Andrews,<sup>†</sup> Jesse G. Zalatan,<sup>‡</sup> and Daniel Herschlag<sup>\*,§</sup>

<sup>†</sup>Department of Chemical and Systems Biology, <sup>‡</sup>Department of Chemistry, and <sup>§</sup>Department of Biochemistry, Stanford University, Stanford, California 94305-5307, United States

## S Supporting Information

**ABSTRACT:** Catalytic promiscuity, the ability of enzymes to catalyze multiple reactions, provides an opportunity to gain a deeper understanding of the origins of catalysis and substrate specificity. Alkaline phosphatase (AP) catalyzes both phosphate and sulfate monoester hydrolysis reactions with a  $\sim 10^{10}$ -fold preference for phosphate monoester hydrolysis, despite the similarity between these reactions. The preponderance of formal positive charge in the AP active site, particularly from three divalent metal ions, was proposed to be responsible for this preference by providing stronger electrostatic interactions with the more negatively charged phosphoryl group versus the sulfuryl group. To test whether positively charged metal ions are required to achieve a high preference for the phosphate monoester hydrolysis reaction, the catalytic preference of three protein tyrosine phosphatases (PTPs), which do not contain metal ions, were measured. Their preferences ranged from  $5 \times 10^6$  to  $7 \times 10^7$ , lower than that for AP but still substantial, indicating that metal ions and a high preponderance of formal positive charge within the active site are not required to achieve a strong catalytic preference for phosphate monoester over sulfate monoester hydrolysis. The observed ionic strength dependences of  $k_{\text{cat}}/K_M$  values for phosphate and sulfate monoester hydrolysis are steeper for the more highly charged phosphate ester with both AP and the PTP Stp1, following the dependence expected based on the charge difference of these two substrates. However, the dependences for AP were not greater than those of Stp1 and were rather shallow for both enzymes. These results suggest that overall electrostatics from formal positive charge within the active site is not the major driving force in distinguishing between these reactions and that substantial discrimination can be attained without metal ions. Thus, local properties of the active site, presumably including multiple positioned dipolar hydrogen bond donors within the active site, dominate in defining this reaction specificity.



Many enzymes exhibit the ability to catalyze, at a low level, the native reactions of related enzymes. This catalytic promiscuity likely played a role in the evolution of new enzymes, and comparisons of promiscuous activities within a set of related enzymes provides an opportunity to learn about the enzymatic features and properties used to optimize catalysis of the cognate reaction.<sup>1–4</sup>

Members of the alkaline phosphatase superfamily catalyze both phosphoryl and sulfuryl transfer reactions but with substantially different catalytic preferences (Table S1, Supporting Information).<sup>5–11</sup> While these two reactions proceed through similar, negatively charged, trigonal bipyramidal transition states (Figure 1), alkaline phosphatase (AP) from *Escherichia coli*, the superfamily's namesake, has a  $10^{10}$ -fold preference for hydrolyzing *p*-nitrophenyl phosphate (pNPP) over *p*-nitrophenyl sulfate (pNPS) (Table 1).<sup>12</sup> In contrast, an aryl sulfatase in the AP superfamily has the opposite preference, catalyzing pNPS hydrolysis with a  $\sim 10^6$ -fold preference over pNPP hydrolysis.<sup>11</sup> Thus, the specificity differential of AP and aryl sulfatase is  $\sim 10^{16}$ -fold, but the origins of the extensive differential specificity in the AP superfamily are not understood.

A simple model for how AP achieves preferential stabilization of the phosphoryl group transition state over the sulfuryl group transition state is that the preponderance of formal positive charge from three metal ions and Arg166 in the AP active site (Figure 2A) is well suited to distinguish differences in negative charge between the phosphoryl group and sulfuryl group transition states.<sup>13</sup> As shown in Figure 1A, a phosphate monoester substrate carries a  $-2$  charge while a sulfate monoester ester substrate carries only a  $-1$  charge. The additional negative charge on the phosphate monoester substrate presumably results in more negative charge on the nonbridging oxygen atoms of the phosphoryl group transition state compared with the sulfuryl group transition state (Figure 1B). The greater negative charge on the phosphoryl group transition state could therefore lead to stronger electrostatic interactions with the positively charged groups in the AP active site, compared with the corresponding weaker electrostatic

Received: June 19, 2014

Revised: October 9, 2014

Published: October 9, 2014

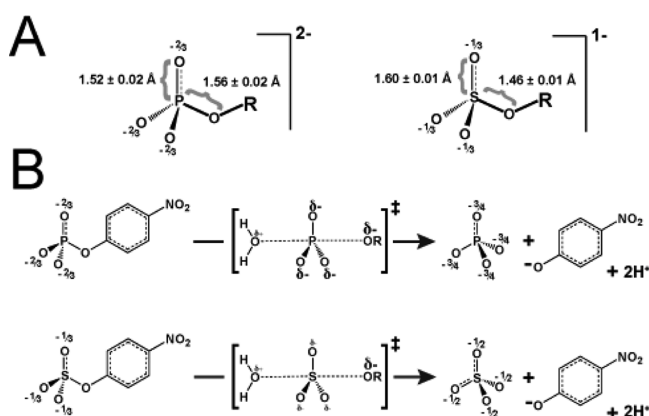


**Figure 1.** Phosphate and sulfate monoesters and their transition states. (A) Comparison of phosphate and sulfate monoesters. Bond lengths are for ethyl phosphate and ethyl sulfate.<sup>50–52</sup> (A comparison of bond lengths for the *p*-nitrophenyl esters is not possible because no structure is available for pNPS.) The apparent ground state negative charge reported for each nonbridging oxygen atom was calculated by dividing the total charge of the molecule by the number of nonbridging oxygen atoms. (B) The solution hydrolysis reactions of pNPP and pNPS both involve nucleophilic attack by water and loose transition state structures in which there is little bond formation with the incoming nucleophile and extensive bond cleavage of the leaving group.<sup>13,31–39</sup> The size of the “ $\delta^-$ ” symbols is meant to qualitatively reflect the relative charge distribution in the transition states.

interactions with the sulfur group. Such preferential electrostatic interactions would lead to greater stabilization and preferential catalysis of the more negatively charged phosphoryl group transition state. Consistent with this model, a previous study with AP demonstrated that catalytic activity increases sharply for a series of substrates with increasing negative charge on the nonbridging oxygen atom situated between the  $\text{Zn}^{2+}$  ions of the bimetallo cluster.<sup>13</sup>

To test whether extensive positive charge, particularly from metal ions as found in the AP active site, is necessary to achieve a strong preference for catalyzing phosphate monoester over sulfate monoester, we turned to a different family of phosphatases. Protein tyrosine phosphatases (PTPs) lack

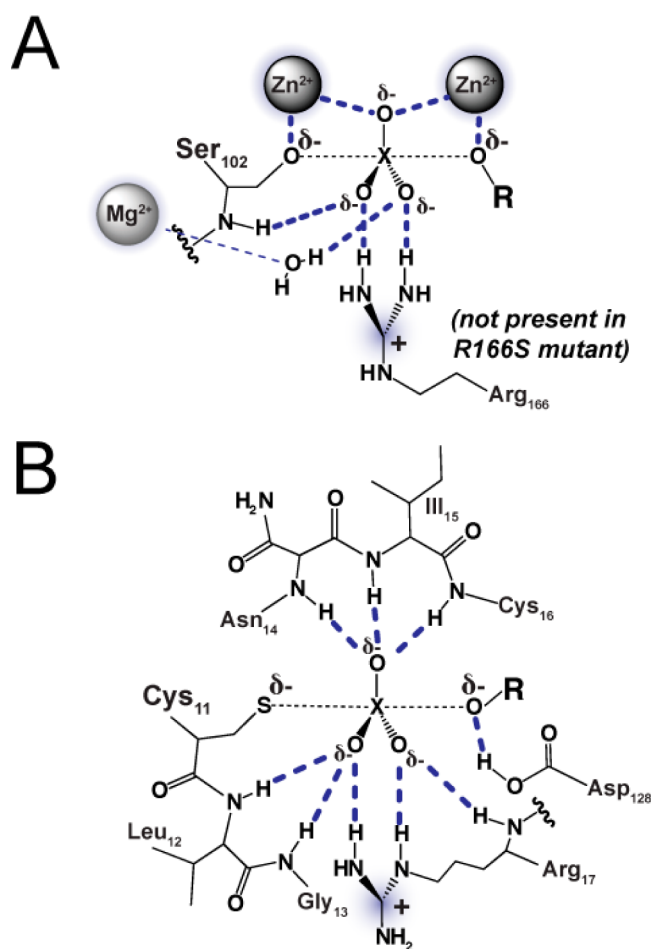


**Figure 2.** Active site schematic for AP (A) and Stp1 (B) with the expected interactions (dark blue dashes) in the transition state for phosphoryl or sulfuryl transfer from a monoester. The central phosphorus or sulfur atom is denoted by an X. Positively charged active site groups are shaded. The schematic for AP is based on the X-ray structure in ref 57 (PDB code 3TG0). The schematic for Stp1 is based on the X-ray structure of low-molecular weight bovine PTP in ref 56 (PDB code 1Z12). The bovine PTP is highly homologous to Stp1 (47% identity) and shares identical active site residues.

**Table 1. Phosphatase and Sulfatase Activity of AP Mutants and PTPs**

	$k_{\text{cat}}/K_M$ ( $\text{M}^{-1} \text{s}^{-1}$ ) <sup>a</sup>		rate enhancement <sup>b</sup>		discrimination <sup>c</sup>
	pNPP	pNPS	pNPP	pNPS	
AP					
WT <sup>d</sup>	$3.3 \times 10^7$ ( $5.8 \times 10^8$ )	$2.8 \times 10^{-3}$	$\geq 7 \times 10^{17}$ ( $1 \times 10^{19}$ )	$3 \times 10^8$	$\geq 2 \times 10^9$ ( $3 \times 10^{10}$ )
R166S <sup>e</sup>	$1.0 \times 10^5$	$6.8 \times 10^{-5}$	$2 \times 10^{15}$	$8 \times 10^6$	$3 \times 10^8$
PTP					
Stp1	$2.6 \times 10^{4f}$	$5.3 \times 10^{-5}$	$2 \times 10^{14}$	$3 \times 10^6$	$7 \times 10^7$
PTP1B	$9.3 \times 10^{4g}$	$1.1 \times 10^{-3}$	$8 \times 10^{14}$	$6 \times 10^7$	$1 \times 10^7$
Yop <sup>51</sup> Δ162	$1.6 \times 10^{5h}$	$3.2 \times 10^{-3}$	$1 \times 10^{15}$	$2 \times 10^8$	$5 \times 10^6$

<sup>a</sup>See Materials and Methods for kinetic assay conditions. <sup>b</sup>Rate enhancement =  $(k_{\text{cat}}/K_M)/k_w$ ;  $k_w$  is the second-order rate constant for attack of water on the monoester. The  $k_w$  value for pNPP hydrolysis was determined<sup>31</sup> at 39 °C and corrected to 25 °C ( $5 \times 10^{-11} \text{ M}^{-1} \text{s}^{-1}$ ), the temperature at which the AP assays were conducted, and 30 °C ( $1.2 \times 10^{-10} \text{ M}^{-1} \text{s}^{-1}$ ), the temperature at which the PTP assays were conducted, using the reported temperature dependence.<sup>31</sup> The  $k_w$  value for pNPS hydrolysis at 25 °C ( $9 \times 10^{-12} \text{ M}^{-1} \text{s}^{-1}$ ) and 30 °C ( $1.7 \times 10^{-11} \text{ M}^{-1} \text{s}^{-1}$ ) was corrected from the value<sup>35</sup> at 35 °C by using the reported temperature dependence.<sup>35</sup> <sup>c</sup>Discrimination = (rate enhancement pNPP)/(rate enhancement pNPS). <sup>d</sup>The rate constant for pNPP hydrolysis by WT and mutant AP was used to estimate the expected second-order rate constant shown in parentheses for the enzymatic reaction with the chemical step rather than diffusion rate limiting, as described in Text S1, Supporting Information.<sup>5</sup> The rate constant for WT AP pNPS hydrolysis was measured here using a discontinuous assay (see Materials and Methods) and agrees well with the previously published value.<sup>12</sup> <sup>e</sup>Values are from a literature source.<sup>7</sup> <sup>f</sup>Within error of the previously reported value of  $3.0 \times 10^4 \text{ M}^{-1} \text{s}^{-1}$ .<sup>14</sup> <sup>g</sup>Within error of the previously reported value of  $1.0 \times 10^5$ .<sup>49</sup> <sup>h</sup>Within error of the previously reported value of  $1.3 \times 10^5 \text{ M}^{-1} \text{s}^{-1}$ .<sup>16</sup>

positively charged metal ions in their active sites (cf. to AP in Figure 2), but their preference for phosphate monoester over sulfate monoester catalysis is unknown. A prediction from the above model of substrate discrimination is that the PTPs would have much less of a preference for phosphate monoester hydrolysis, given the paucity of positively charged groups in their active sites. Contrary to this prediction, our results show that PTPs provide robust discrimination. These and additional results suggest that positively charged metal ions or a high formal positively charged active site is not needed to achieve a high degree of discrimination.

## MATERIALS AND METHODS

**Materials.** All chemicals including substrates, buffers, and salts were obtained from commercial sources and were reagent grade. Site-directed mutants were prepared using a Quik-Change site-directed mutagenesis kit (Stratagene).

**Protein Expression and Purification.** The expression and purification of Stp1 was conducted based on a previous protocol.<sup>14</sup> Briefly, *E. coli* BL21(DE3) cells containing plasmid pT7-7 with the Stp1 sequence were grown to OD<sub>600</sub> 0.6–0.9 in 2XYT media (5 g of NaCl, 16 g of tryptone, 10 g of yeast extract per liter) and induced with 0.4 mM IPTG for 4–5 h. Cells were pelleted, resuspended in buffer A (20 mM Na acetate, pH 5.1, 100 mM NaCl, and 1 mM EDTA), and lysed by passage through a French press or high-pressure homogenizer. Following centrifugation, the supernatant was filtered through a 0.2  $\mu$ m membrane (Nalgene) and subjected to FPLC ion exchange chromatography (HiPrep 16/10 CM Sepharose, 20 mL column, flow rate 5 mL/min, at 4 °C), washed with 200 mL of buffer A, and eluted by flowing a gradient from 100% buffer A to 100% buffer B (20 mM Na acetate, pH 5.1, 500 mM NaCl, and 1 mM EDTA) over 200 mL. Fractions containing protein, as determined by absorbance at 280 nm, were pooled, concentrated to ~1 mL, and passed through (at 0.9 mL/min) a gel filtration column (Superose-12 column, 100 mL column). Typical protein yields were >15 mg/L. Purity was estimated to be >95% from band intensities of Coomassie Blue-stained SDS-polyacrylamide gels. Protein concentration was determined by absorbance at 280 nm in 6 M guanidine hydrochloride and 20 mM sodium phosphate, pH 6.5, using a calculated extinction coefficient of 12110 M<sup>-1</sup> cm<sup>-1</sup>.

Human PTP1B contained in the pT7-plasmid was overexpressed and purified according to a previously published protocol.<sup>15</sup> Purity was estimated to be >95% by SDS-PAGE, and the concentration was determined as above using a calculated extinction coefficient of 59560 M<sup>-1</sup> cm<sup>-1</sup>.

Yop<sup>51</sup>\* $\Delta$ 162, a PTP from *Yersinia pestis* having a C235R point mutation and lacking the N-terminal 162 amino acids that is catalytically equivalent to the full length protein, was overexpressed and purified as described previously.<sup>16</sup> Purity was estimated to be >95% by SDS-PAGE, and the concentration was determined as above using a calculated extinction coefficient of 15965 M<sup>-1</sup> cm<sup>-1</sup>.

The R166S mutant of AP was purified as described previously.<sup>17</sup> Purity was estimated to be >95% by SDS-PAGE, and the concentration was determined by absorbance at 280 nm in 6 M guanidine hydrochloride and 20 mM sodium phosphate, pH 6.5, using a calculated extinction coefficient of 31390 M<sup>-1</sup> cm<sup>-1</sup>. The concentration of R166S AP was also confirmed by activity assays using 1 mM pNPP and agreed with previously reported  $k_{cat}$  values within 20%.<sup>18</sup>

**Kinetic Methods.** Standard reaction conditions for the PTPs (WT and C11G Stp1, PTP1B, and Yop<sup>51</sup>\* $\Delta$ 162) were 20 mM Na maleate, pH 6.0, 0.15 M NaCl, 0.1 mM EDTA, and 30 °C. Phosphatase activity toward pNPP was followed in quartz cuvettes (1 mL) by measuring the appearance of the *p*-nitrophenolate product (extinction coefficient of 1635 M<sup>-1</sup> cm<sup>-1</sup> at pH 6.0) using a Uvikon 9310 or PerkinElmer  $\lambda$ -25 UV–vis spectrophotometer. Rate constants were obtained from initial rates (typically  $\leq$ 5% reaction). Reactions were shown to be first order in substrate and enzyme by varying substrate and enzyme over a >10-fold range. Replicate measurements gave rate constants that varied by  $\leq$ 10%.

Sulfatase activity toward pNPS was followed by the appearance of the *p*-nitrophenolate product using a discontinuous assay.<sup>19</sup> Appearance of the phenolate was monitored by removing aliquots from the reaction, quenching in a relatively small volume of 1 M NaOH, and measuring the absorbance at 400 nm (with background subtraction at 500 nm to control for instrument drift over the long time periods required to measure the sulfatase activity). The example sulfatase assay results for Stp1 in Figure S1, Supporting Information, were also repeated using ~2-fold lower enzyme concentration (Figure S1, Supporting Information) to demonstrate that the reaction velocity was proportional to the concentration of enzyme as expected. Replicate measurements with Stp1 gave rate constants that varied by  $\leq$ 25%. This discontinuous assay approach was also validated by using it to follow the phosphatase activity of Stp1 to reproduce the kinetic parameters obtained from the standard assay in which product generation is followed continuously.

The measurement of the R166S AP phosphatase and sulfatase activities was conducted as reported previously<sup>12,13</sup> in the standard reaction conditions of 100 mM NaMOPS, pH 8.0, 100 mM NaCl, 1 mM MgCl<sub>2</sub>, 100  $\mu$ M ZnCl<sub>2</sub>, and 30 °C.

**Inhibition Measurements.** To test whether the observed sulfatase activity was due to Stp1 and not contamination by a small quantity of a proficient sulfatase enzyme, the inhibition constant for P<sub>i</sub> was measured by varying the inhibitor concentration at least 10-fold below and above the observed  $K_i$  at constant enzyme concentrations and constant, subsaturating concentrations of either pNPP or pNPS in the standard reaction conditions listed above. For inhibition of the phosphatase activity reactions contained 20 nM Stp1 and 50  $\mu$ M pNPP. For inhibition of the sulfatase activity reactions contained 390  $\mu$ M WT Stp1 and 1 mM pNPS. Initial velocities for both activities at each concentration of P<sub>i</sub> were determined by linear least-squares fits. The inhibition constant was determined by nonlinear least-squares fits using the appropriate equation for competitive inhibition.

The inhibition data for PTP1B and Yop<sup>51</sup>\* $\Delta$ 162 are shown in Figure S3, Supporting Information. For these enzymes, the inhibitor, inorganic arsenate, was used instead of P<sub>i</sub> because the P<sub>i</sub> inhibition of these enzymes is weak (>10 mM) and difficult to measure accurately for both phosphatase and sulfatase activities. For inhibition of the PTP1B phosphatase activity, reactions contained 10 nM PTP1B and 100  $\mu$ M pNPP. For inhibition of the PTP1B sulfatase activity reactions contained 20  $\mu$ M PTP1B and 5 mM pNPS. For inhibition of the Yop<sup>51</sup>\* $\Delta$ 162 phosphatase activity reactions contained 20 nM Yop<sup>51</sup>\* $\Delta$ 162 and 300  $\mu$ M pNPP. For inhibition of the Yop<sup>51</sup>\* $\Delta$ 162 sulfatase activity reactions contained 30  $\mu$ M Yop<sup>51</sup>\* $\Delta$ 162 and 2 mM pNPS. Initial velocities at each concentration of arsenate were determined by linear least-



squares fits. The inhibition constants were determined by nonlinear least-squares fits using the equation for competitive inhibition (see Figure S3, Supporting Information, legend).

**Ionic Strength Dependencies.** Assays for *p*NPP and *p*NPS hydrolysis by R166S AP were conducted in 5 mM NaMOPS, pH 8.0, at 30 °C with 0–800 mM NaCl, except for controls with alternative salts (see Results and Discussion). Assays for Stp1 were conducted in 5 mM Na maleate, pH 6.0, at 30 °C with the same NaCl concentrations and alternative salts.

The observed ionic strength dependencies were insensitive to the concentration of substrate when the substrate concentration was maintained at least 2-fold below the expected  $K_M$  value. With substrate concentrations significantly above the  $K_M$ , the substrate-binding step no longer contributes to the observed activity. Under such conditions, electrostatic forces subject to electrostatic screening from increasing ionic strength are not expected to contribute to the observed activity. Consistent with this expectation, the observed activity for *p*NPP hydrolysis by R166S AP and Stp1 did not change with ionic strength when the *p*NPP concentration was well above the expected  $K_M$  (Figure S7, Supporting Information).

The ionic strength of the assay solutions includes contributions from the buffer and was computed using  $I = 0.5 \sum c_i z_i^2$ , where  $I$  is the ionic strength,  $c_i$  is the ion molarity of ion  $i$ , and  $z_i$  is the charge number of that ion.

## RESULTS AND DISCUSSION

**Catalytic Discrimination by Protein Tyrosine Phosphatases (PTPs) between Phosphate and Sulfate Monoester Hydrolysis.** To determine the catalytic discrimination of a PTP, we first measured the phosphatase activity of the PTP Stp1. Our value for  $k_{cat}/K_M$  for the hydrolysis of the phosphate monoester, *p*NPP, of  $2.6 \times 10^4 \text{ M}^{-1} \text{ s}^{-1}$  (Table 1), agrees with previous measurements with this substrate.<sup>14,20</sup> This value corresponds to a rate enhancement over the uncatalyzed reaction rate constant,  $k_w$ , of  $(2.2 \times 10^{14})$ -fold  $[= (k_{cat}/K_M)/k_w]$  (Table 1). Our Stp1 preparation also exhibited *p*NPS hydrolysis activity, with  $k_{cat}/K_M = 5.3 \times 10^{-5} \text{ M}^{-1} \text{ s}^{-1}$  (Figure S1, Supporting Information; Table 1). Although this  $k_{cat}/K_M$  value is very low compared with physiological activities, even with the activated *p*-nitrophenolate leaving group, it nonetheless would correspond to a substantial rate enhancement above the uncatalyzed reaction of more than a million-fold (Table 1).

Low observed promiscuity, however, raises the concern that the observed activity could be due to a very low concentration of a contaminating enzyme with a high activity for the promiscuous reaction, in this case, sulfate monoester hydrolysis. As carried out previously for AP and its mutants,<sup>12,17,21</sup> several controls can be used to test whether Stp1 is responsible for the observed sulfatase activity and whether the reaction occurs in the Stp1 active site. First, we showed that multiple Stp1 preparations had the same activity, within error (Figure S1, Supporting Information). Thus, any potential contamination would have to be constant between protein preparations. Second, we showed that inorganic phosphate ( $P_i$ ), a competitive inhibitor of Stp1, inhibits the phosphatase and sulfatase activities with the same inhibition constant (Figure 3A), suggesting that both activities arise from a common active site. Further, because the sulfatase activity is several orders of magnitude lower than the phosphatase activity, the *p*NPS substrate does not react significantly on the time scale of the

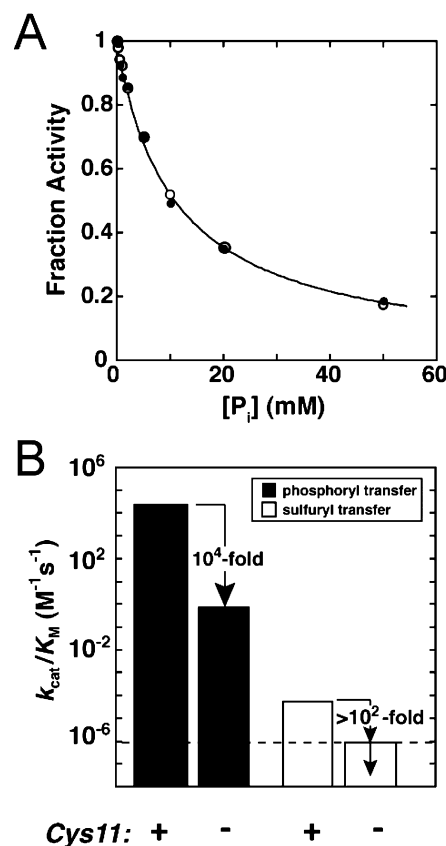


**Figure 3.** Evidence that the observed promiscuous sulfatase activity arises from PTP. (A) Coincident inhibition of phosphatase (*p*NPP hydrolysis, filled circles) and sulfatase (*p*NPS hydrolysis, open circles) activities by inorganic phosphate ( $P_i$ ) (see Materials and Methods for assay conditions). For comparison, activity was normalized by dividing the observed rate constant in the presence of inhibitor by the rate constant in the absence of inhibitor. The line represents a nonlinear least-squares fit to the combined data for competitive inhibition of both activities and gave an inhibition constant of  $K_i = 11.0 \pm 0.3 \text{ mM}$ . Individual fits to the phosphatase and sulfatase data gave values of  $K_i$  that are the same within error ( $10.9 \pm 0.6$  and  $11.1 \pm 0.2$ , respectively). (B) Phosphatase and sulfatase activity of Stp1 with and without the intact Cys11 nucleophile. Assay conditions are described in the Materials and Methods. The dotted line shows the detection limit for sulfatase activity. The sulfatase activity of C11G Stp1 is below this detection limit. Also, there is no evidence that the remaining very low activities arise from the mutated Stp1 as opposed to contaminating activities present at extremely low levels.

phosphatase reaction. We could therefore determine whether *p*NPS inhibits *p*NPP activity with a  $K_i$  value corresponding to the  $K_M$  value observed for *p*NPS hydrolysis (Table S1, Supporting Information), as would be expected for reaction from the same enzyme and active site. The inhibition constant for *p*NPS inhibition was within error of the observed  $K_M$  value for *p*NPS hydrolysis (Figure S2 and Table S2, Supporting Information). Finally, we showed that mutation of the active site nucleophile from cysteine to glycine substantially decreases both the phosphatase and sulfatase activities (Figure 3B), providing strong evidence that both reactions are catalyzed by Stp1 and occur within the same active site.

These results strongly suggest that the observed sulfatase activity arises from the Stp1 active site. Comparison of the Stp1 phosphatase and sulfatase activities gives a discrimination of 7

$\times 10^7$ -fold (determined as the ratio of rate enhancements for the *p*NPP and *p*NPS hydrolysis reactions; Table 1).

To determine whether the extent of discrimination by Stp1 generalizes to other PTPs, we measured the *p*NPS activity of PTP1B and Yop<sup>S1</sup>\* $\Delta$ 162, which have conserved active site features that are found in Stp1: a cysteine nucleophile, an arginine in position to contact the nonbridging oxygen atoms of the substrate, and a general acid that protonates the monoester leaving group (Figure 2B).<sup>22,23</sup> The catalytic domains of these PTPs also share significant overall sequence identity.<sup>22,24–26</sup>

Sulfatase activity was detected for both PTPs (Table 1). The phosphatase and sulfatase activities of each of the two PTPs were inhibited equally by inorganic arsenate, providing evidence that both activities are catalyzed by the PTPs and take place in the same active site (Figure S3, Supporting Information). As shown in Table 1, these PTPs exhibit discrimination within  $\sim 10$ -fold of Stp1, suggesting that the conserved features of the PTP active site are responsible for the similar catalytic preferences for phosphate over sulfate ester hydrolysis.

**Comparison of the Catalytic Discrimination of AP and PTPs.** The three PTPs tested preferentially catalyze phosphate ester over sulfate ester hydrolysis by  $(0.5\text{--}7) \times 10^7$ -fold (Table 1). This discrimination is  $\sim 100$ -fold less than the discrimination of  $2 \times 10^9$  observed for AP (Table 1), and the AP value is an underestimate of the discrimination in the chemical transition state, because substrate binding is rate-limiting for *p*NPP reacting with wild-type AP.<sup>27–30</sup> Several comparisons suggest that the actual discrimination between the chemical transition states for the AP phosphatase and sulfatase reactions is  $\sim 3 \times 10^{10}$  (Table 1; Text S1, Supporting Information), which corresponds to an overall  $\sim 1000$ -fold greater discrimination by AP than by the PTPs.

On the surface, these results might suggest a considerable contribution to discrimination from the AP metal ions. However, the PTP active sites that lack metal ions provide  $\sim 10^7$ -fold discrimination, and mutation of AP to remove its active site arginine residue (R166) leaves all three active site metal ions unaffected<sup>18</sup> but reduces the phosphatase/sulfatase discrimination to  $3 \times 10^8$ , within 10-fold of the discrimination achieved by a metal-free PTP (Table 1).

**Testing Possible Origins of the Observed Catalytic Discrimination by AP and PTPs.** The results above indicate that substantial discrimination between phosphate and sulfate esters of greater than a million fold can be achieved without the involvement of metal ion interactions and in active sites with little formal positive charge. To test whether there might nevertheless be a similar overall electrostatic component to discrimination by AP and the PTPs such that a strong long-range electrostatic attraction was felt for more highly charged substrates to both AP and PTP active sites, we compared the ionic strength dependences of each enzyme with the phosphate monoester dianion and sulfate monoester monoanion substrates.

Calculation of the surface electrostatic potentials for AP and Stp1 using a Poisson–Boltzmann equation solver reveal positive potentials near the active sites (Figure 4) that could contribute to discrimination by preferentially attracting more negatively charged substrates into the active site and thereby favor formation of the enzyme and substrate complex for the more highly charged substrate. If a long-range attractive electrostatic potential contributes to the AP and Stp1 catalyzed reactions, the presence of counterions would be expected to

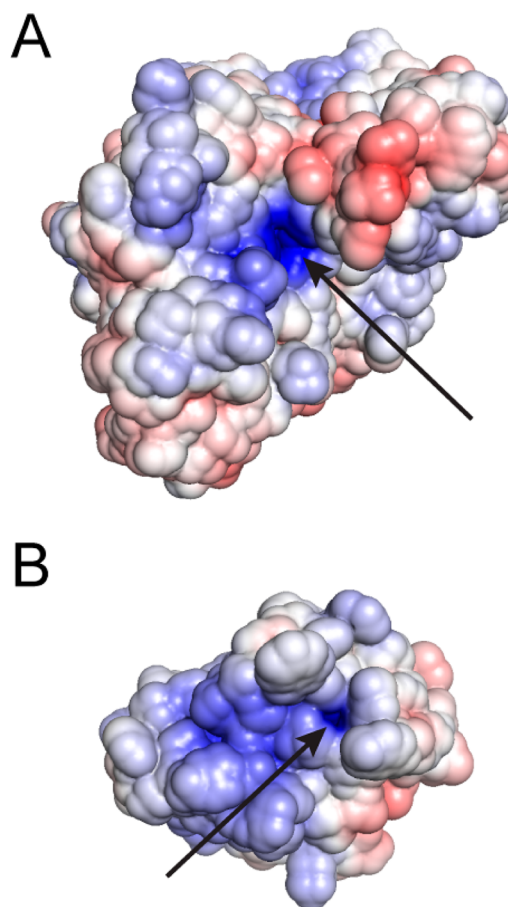


**Figure 4.** Models of the electrostatic surface potential for WT AP (A) and Stp1 (B) with arrows pointing to the active site nucleophile. For modeling AP, the X-ray structure from ref 57 was used (PDB code 3TG0). For modeling Stp1, the X-ray structure of low-molecular weight bovine PTP in ref 56 (PDB code 1Z12) was used to generate a structural homology model of Stp1 using the program Modeller.<sup>53</sup> The protein surface is colored according to electrostatic potential (positive, blue; negative, red;  $\pm 6kT/e$ ). For the electrostatic calculation, the active site nucleophiles of AP and Stp1 were deprotonated, and for Stp1, the Asp28 general acid was protonated. Created with AMBER/ABPS in MacPyMOL.<sup>54,55</sup>

decrease this attraction so that the catalytic activity would decrease as the ionic strength of the reaction solution is raised and decrease more for a more highly charged enzyme. Because increased ionic strength will screen long-range charge–charge interactions and not local interactions, this experiment cannot probe local electrostatic and dipolar interactions that are within the active site and involved in the progression from the enzyme/substrate to the enzyme/transition state complex. In addition, because nonideal effects of ions on enzymes are common, comparison of the ionic strength dependence of reactions of the (phosphate ester) dianion versus (sulfate ester) monoanion substrates for each enzyme is important in controlling for such effects.

The ionic strength dependencies of activity for AP and Stp1 are shown in Figure 5A,B, respectively. The *p*NPP hydrolysis activity of WT AP is limited by diffusion rather than the chemical step.<sup>27–30</sup> To allow for a consistent comparison of ionic strength dependent activity, R166S AP was used in Figure 5A because neither its *p*NPP nor its *p*NPS reaction is diffusion-limited<sup>13,18</sup> so that the binding and hydrolysis steps contribute

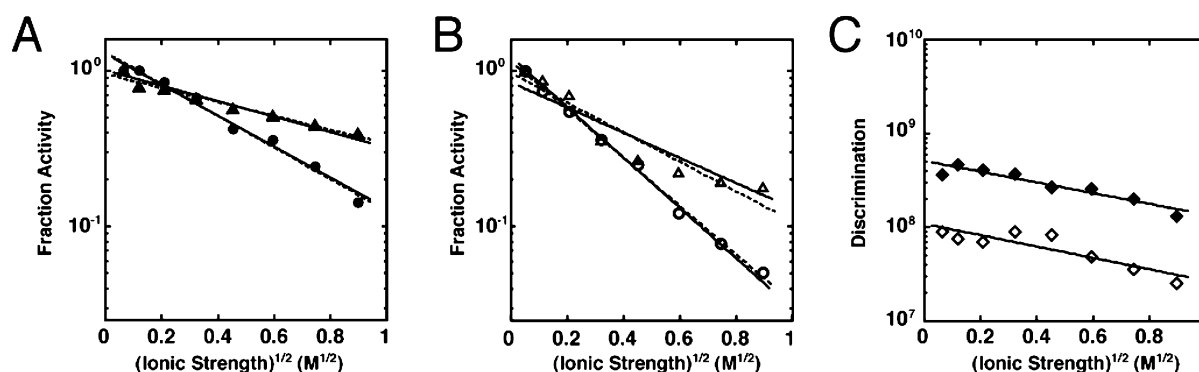


**Figure 5.** Ionic strength dependencies for the hydrolysis of *p*NPP (circles) and *p*NPS (triangles) by R166S AP (A) and Stp1 (B). See Materials and Methods for assay conditions. For comparison, fraction activity was calculated by dividing each observed rate constant by the rate constant measured at the lowest ionic strength measured. The slope  $[\log(\text{fraction activity})/(\text{ionic strength})^{1/2}]$  provides an estimate for the product of the interacting charges of substrate ( $Z_0$ ) and the enzyme ( $Z_{\text{enz}}$ ) according to the Debye–Hückel equation  $\log(\text{fraction activity}) = 2AZ_0Z_{\text{enz}}(\text{ionic strength})^{1/2} + C$ , where  $A$  is 0.516 at 30 °C,  $C$  is the fraction activity as the ionic strength approaches zero ( $C = 1.30$  and  $1.01$  for *p*NPP and *p*NPS in panel A and  $1.23$  and  $0.85$  for these two substrates in panel B); and  $Z_0$  is fixed at  $-2$  for the *p*NPP data and at  $-1$  for the *p*NPS data. Solid lines show global best fits, and dashed lines show individual best fits and yield  $Z_{\text{enz}}$  values reported in Table 2. (C) The discrimination of *p*NPP hydrolysis activity over *p*NPS hydrolysis activity for R166S AP (filled diamonds) and Stp1 (open diamonds). Solid lines show the best fits to the linear Debye–Hückel model treating the value of the slope as a variable. The y-axis is on a logarithmic scale.

to the observed hydrolysis activities for both substrates. Although R166S AP contains one less active site positive charge than WT AP, the active site of R166S AP still contains five more formal positive charges than the Stp1 active site and its calculated electrostatic surface potential map also suggests significant positive potential near the surface of the active site entrance (Figure S4D, Supporting Information).

Ionic strength dependencies can also be complicated by direct binding of ions to the active site or by ionic-strength dependent changes in active site conformations of the enzyme. Control reactions, using KCl or NaBr to test for ion-specific effects, gave essentially the same dependencies as that with NaCl for both AP and Stp1 (Figure S5, Supporting Information), as expected for effects arising from electrostatic screening in the absence of specific binding. In addition, if the ionic strength dependence were due to the screening of electrostatic potential between the substrate and active site, the steepness of the dependence would be predicted to be proportional to the formal charge of the reactants, that is, the absolute charge of the substrate and the enzyme. Fitting the ionic strength dependent data gives a slope for the *p*NPP hydrolysis activity that is two times greater than the corresponding slope of the *p*NPS activity for both R166S AP (Figure 5A) and Stp1 (Figure 5B), as expected from the charge differential of the two substrates. This differential dependence of *p*NPP and *p*NPS hydrolysis strongly suggests that the ionic strength dependencies reflect screening of electrostatic potential between the active site and substrate.

With these controls in hand, we set out to assess potential electrostatic differences between the enzymes that could contribute to reactions starting from free enzyme and free substrate. Because the R166S AP active site contains six formal positive charges, compared with the Stp1 active site's single formal positive charge, it might have been expected that the decrease in activity for a given change in ionic strength would be much greater for the R166S AP-catalyzed reactions. However, this was not the case. Indeed, the dependence for Stp1 with each substrate was steeper than that for R166S AP (Figure 5; cf. parts A and B). These slopes can be converted, according to a simple Debye–Hückel formalism, into apparent

overall charges of the enzyme, which give, as expected based on the differential steepness, a larger value for Stp1 than for R166S AP (Table 2).

**Table 2. Effective Enzyme Charge for R166S AP and Stp1 Determined by the Ionic Strength Dependence of Activity<sup>a</sup>**

	$Z_{\text{enz}}$		
	<i>p</i> NPP ( $Z_0 = -2$ )	<i>p</i> NPS ( $Z_0 = -1$ )	global fit
R166S AP	$+0.49 \pm 0.03$	$+0.43 \pm 0.03$	$+0.48 \pm 0.02$
Stp1	$+0.75 \pm 0.02$	$+0.92 \pm 0.12$	$+0.78 \pm 0.08$

<sup>a</sup>Values of the effective ionic charge of the enzyme,  $Z_{\text{enz}}$ , were determined from fits to the Debye–Hückel equation to the ionic strength dependent data in Figure 4A,B.

We next wanted to calculate the ionic strength dependence for the discrimination by each enzyme and to compare them. Because no significant ionic strength dependence is observed for the uncatalyzed rates of hydrolysis of *p*NPP or *p*NPS (Figure S6, Supporting Information), the catalytic discrimination at each ionic strength can be determined from the ratios of rate constants in Figure 5A,B for R166S AP and Stp1, respectively. This discrimination, shown in Figure 5C, is only modestly affected, and the effect is nearly the same for the two enzymes: for a change in ionic strength from 0.004 to 0.8 M, the discrimination changes only ~3-fold for both enzymes (2.8- and 3.5-fold for R166S AP and Stp1, respectively). At the highest ionic strength shown in Figure 5C (0.8 M),  $10^{8.1}$ -fold discrimination remains for R166S AP and  $10^{7.4}$ -fold discrimination remains for Stp1.

## CONCLUSIONS AND IMPLICATIONS

The discrimination of AP between its cognate phosphate monoester dianion and noncognate sulfate monoester monoanion reactions is very high,  $\geq 2 \times 10^9$ -fold, and estimated to be  $\sim 3 \times 10^{10}$  (Table 1; Text S1, Supporting Information). We have shown that this discrimination is not uniquely a function of the high formal charge density of its active site, because the PTPs tested, which have only one positively charged active site group instead of the +7 formal positive charges in the AP active



site, also exhibited high levels of discrimination,  $(0.5-7) \times 10^7$ -fold (Table 1; Figure 2). Removal of the single nonmetal ion positive charge from AP, to give the R166S mutant, reduced discrimination to  $3 \times 10^8$ , similar to that for the PTPs, despite the remaining six positive charges from AP's three active site divalent metal ions.

Increasing the concentration of ions in solution had only modest effects on the discrimination between the dianionic and monoanionic substrates. Thus, the formal charges of the AP metal ions are apparently sufficiently balanced by the anionic metal ion ligands and other negatively charged groups such that there is no large global electrostatic attraction between free enzyme and free substrate that accounts for the bulk of the observed discrimination for AP.

The factor or factors involved in discrimination by AP and by PTPs remain to be elucidated. We briefly note potential factors and then close by noting a striking correlation between discrimination and overall rate enhancement.

Differential catalysis via differential nucleophile activation and leaving group stabilization could contribute to greater phosphatase than sulfatase activity. However, the transition states for phosphoryl and sulfonyl transfer are indistinguishable,<sup>4</sup> both in solution<sup>13,31-39</sup> and at the AP active site, as assessed by leaving group <sup>18</sup>O isotope effects<sup>40,41</sup> (see also ref 42), so that differential catalysis via nucleophile activation and leaving group stabilization would not be expected. Given the larger charge density on the phosphoryl oxygen atoms, relative to the sulfonyl oxygen atoms, stronger hydrogen bond and other local electrostatic interactions, which were not assessed in our experiments, could provide all or some of the observed discrimination. It is also possible that precise arrangement of groups within the AP and PTP active sites allow discrimination despite the very modest geometrical differences of only  $\sim 0.1$  Å (Figure 1).<sup>45-47</sup> Finally, the hydrolysis of phosphate monoester dianions is greatly accelerated in largely organic solvents in the presence of very little water, whereas sulfate monoester monoanion hydrolysis is much less affected so that differential solvation energetics of the ground and transition states in solution and in the enzyme active site need to be considered and may contribute to phosphate ester versus sulfate ester specificity.<sup>44,48</sup> Conversely, we do not understand how sulfatases, which also have a preponderance of charged and polar active site groups, discriminate in favor of sulfate ester hydrolysis over phosphate ester hydrolysis.<sup>11</sup> These observations of reversed discrimination indicate that features beyond simple accounting of potential active site electrostatic interaction energies need to be invoked and dissected in order to understand the observed discriminations and, ultimately, to predict and design binding and catalytic specificity.

**An Intriguing Correlation of Catalytic Efficiency and Discrimination.** Figure 6A shows the phosphate/sulfate monoester discrimination as a function of the catalytic efficiency for hydrolysis of phosphate monoester dianions for all enzymes for which these parameters have been measured of which we are aware. Based on this limited sample set, there is a strong correlation, but it appears that sulfatase activity remains at a similar level (Figure 6B) so that the correlation is driven by increased phosphatase activity; that is, as phosphatase activity is increased, sulfatase activity does not increase commensurately (Figure 6B). Active site features that provide optimal phosphatase catalysis may affect only or predominantly this reaction, or increased catalytic power toward phosphate esters

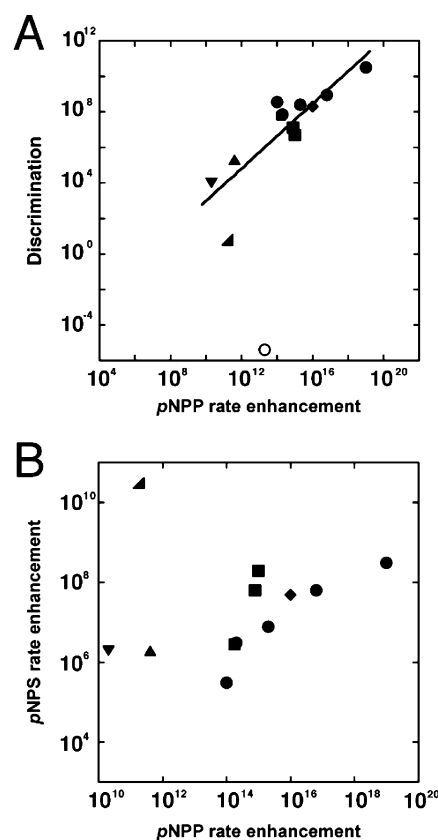


**Figure 6.** Analysis of relative rate enhancements for cognate reactions with their ability to discriminate between phosphate and sulfate ester substrates. (A) Correlation of the enzymatic rate enhancement of *p*NPP hydrolysis with the extent of catalytic discrimination between *p*NPP and *p*NPS hydrolysis by AP superfamily members and PTPs. Data are from results herein and prior studies and are summarized in Table S1, Supporting Information. The linear least-squares fit has a slope of 0.9 log units ( $R^2 = 0.74$ ). Key: circles for AP and mutants thereof; diamond for PAF; squares for PTPs; triangle for PMS; inverted triangle for NPP; right angle triangle for PMH; open circle for PAS. See Table S1, Supporting Information, for enzyme abbreviations. The data point for PAS was not included in the fit because this enzyme prefers to hydrolyze *p*NPS over *p*NPP. (B) Plot of the enzymatic rate enhancement of *p*NPP hydrolysis with the enzymatic rate enhancement of *p*NPS hydrolysis by AP superfamily members and PTPs (excluding the AP superfamily member PAS). Key: same as in panel A). The data point for PAS is omitted to allow better visualization of the other data points but is included in an analogous plot in the Supporting Information (Figure S8).

may be accompanied by selective pressure against also increasing activity for sulfatase side reactions.

A grand challenge will be to reach a sufficient level of understanding to allow enzymes to be designed with catalytic power rivaling those of natural enzymes and with specificity and promiscuity that can be dialed up or down by following a set of engineering principles grounded in physical and chemical understanding.

## ■ ASSOCIATED CONTENT

### Supporting Information

A table of kinetic parameters for PTPs, AP superfamily member enzymes, and mutants thereof, plots of reaction progress curves, Michaelis–Menten curves, and inhibition curves, a discussion of the rate-limiting step for AP hydrolysis of *p*NPP, a

table of PTP kinetic parameters, two-dimensional active site schematics and electrostatic surface potential representations of wild type AP, R166S AP, and wild type PTP, plots of ionic strength dependencies, and a plot of *p*NPP and *p*NPS rate enhancements for AP superfamily members and PTPs. This material is available free of charge via the Internet at <http://pubs.acs.org>.

## AUTHOR INFORMATION

### Corresponding Author

\*Telephone: 650-723-9442. Fax: 650-723-6783. E-mail: [herschla@stanford.edu](mailto:herschla@stanford.edu).

### Funding

This work was supported by a grant from the National Institutes of Health (NIH) to D.H. (GM64798). L.D.A. was supported in part by an NIH training grant (R1GM064798). J.G.Z. was supported in part by a Hertz Foundation Graduate Fellowship.

### Notes

The authors declare no competing financial interest.

## ACKNOWLEDGMENTS

We thank Professor Zhong-Yin Zhang for generously providing PTP expression plasmids. We also thank members of the Herschlag lab for comments on the manuscript.

## ABBREVIATIONS

AP, *E. coli* alkaline phosphatase; PTP, protein tyrosine phosphatase; *p*NPP, *p*-nitrophenyl phosphate; *p*NPS, *p*-nitrophenyl sulfate; KIE, kinetic isotope effect

## ADDITIONAL NOTE

<sup>a</sup>The value of the <sup>18</sup>O isotope effect for the leaving group oxygen atom is identical, within error, for the solution phosphoryl and sulfuryl transfer reactions [KIE for solution reactions of *p*NPP<sup>2-</sup> and *p*NPS<sup>1-</sup> is 1.0189 and 1.0210, respectively].<sup>43,44</sup> The KIE's measured for AP are also identical, as follows. The <sup>18</sup>O IE for R166S AP with *p*NPP is 1.0091 ± 0.0006.<sup>40</sup> (The value for WT AP cannot be used because the chemical step is not rate limiting for this reaction.) This IE is the same as that for the *p*NPS (sulfatase) reaction with WT AP, 1.0084 ± 0.001.<sup>40</sup> [Here WT AP is used because the R166S AP/*p*NPS reaction is too slow to get accurate IEs; We can directly compare WT AP and R166S AP because the presence or absence of R166 does not change the IE, as demonstrated with the substrate *p*NPPS (the phosphorothioate substrate) where the IEs are 1.0094 ± 0.0004 (WT) and 1.0098 ± 0.0003 (R166S).<sup>41</sup>]

## REFERENCES

- Jensen, R. A. (1976) Enzyme recruitment in evolution of new function. *Annu. Rev. Microbiol.* 30, 409–425.
- O'Brien, P. J. (2006) Catalytic promiscuity and the divergent evolution of DNA repair enzymes. *Chem. Rev.* 106, 720–752.
- Aharoni, A., Gaidukov, L., Khersonsky, O., Gould, S. M., Roodveldt, C., and Tawfik, D. S. (2004) The 'evolvability' of promiscuous protein functions. *Nat. Genet.* 37, 73–76.
- Khersonsky, O., and Tawfik, D. S. (2010) Enzyme promiscuity: A mechanistic and evolutionary perspective. *Annu. Rev. Biochem.* 79, 471–505.
- O'Brien, P. J., and Herschlag, D. (2002) Alkaline phosphatase revisited: Hydrolysis of alkyl phosphates. *Biochemistry* 41, 3207–3225.

- Zalatan, J., Fenn, T., Brunger, A., and Herschlag, D. (2006) Structural and functional comparisons of nucleotide pyrophosphatase/phosphodiesterase and alkaline phosphatase: Implications for mechanism and evolution. *Biochemistry* 45, 9788–9803.
- Lassila, J., and Herschlag, D. (2008) Promiscuous sulfatase activity and thio-effects in a phosphodiesterase of the alkaline phosphatase superfamily. *Biochemistry* 47, 12853–12859.
- Berluti, F., Passariello, C., Selan, L., Thaller, M. C., and Rossolini, G. M. (2001) The *Chryseobacterium meningosepticum* PafA enzyme: Prototype of a new enzyme family of prokaryotic phosphate-irrepressible alkaline phosphatases? *Microbiology* 147, 2831–2839.
- Kim, A., Benning, M. M., OkLee, S., Quinn, J., Martin, B. M., Holden, H. M., and Dunaway-Mariano, D. (2011) Divergence of chemical function in the alkaline phosphatase superfamily: Structure and mechanism of the P-C Bond cleaving enzyme phosphonoacetate hydrolase. *Biochemistry* 50, 3481–3494.
- Van Loo, B., Jonas, S., Babbie, A. C., Benjdia, A., Berteau, O., Hyvonen, M., and Hollfelder, F. (2010) An efficient, multiply promiscuous hydrolase in the alkaline phosphatase superfamily. *Proc. Natl. Acad. Sci. U.S.A.* 107, 2740–2745.
- Olguin, L. F., Askew, S. E., O'Donoghue, A. C., and Hollfelder, F. (2008) Efficient catalytic promiscuity in an enzyme superfamily: An arylsulfatase shows a rate acceleration of 10<sup>13</sup> for phosphate monoester hydrolysis. *J. Am. Chem. Soc.* 130, 16547–16555.
- O'Brien, P. J., and Herschlag, D. (1998) Sulfatase activity of *E. coli* alkaline phosphatase demonstrates a functional link to arylsulfatases, and evolutionarily related enzyme family. *J. Am. Chem. Soc.* 120, 12369–12370.
- Nikolic-Hughes, I., O'Brien, P., and Herschlag, D. (2005) Alkaline phosphatase catalysis is ultrasensitive to charge sequestered between the active site zinc ions. *J. Am. Chem. Soc.* 127, 9314–9315.
- Zhang, Z. Y., Zhou, G., Denu, J. M., Wu, L., Tang, X., Mondesert, O., Russell, P., Butch, E., and Guan, K. L. (1995) Purification and characterization of the low molecular weight protein tyrosine phosphatase, Stp1, from the fission yeast *Schizosaccharomyces pombe*. *Biochemistry* 34, 10560–10568.
- Zhang, Y. L., and Zhang, Z. Y. (1998) Low-affinity binding determined by titration calorimetry using a high-affinity coupling ligand: A thermodynamic study of ligand binding to protein tyrosine phosphatase 1B. *Anal. Biochem.* 261, 139–148.
- Zhang, Z. Y., Clemens, J. C., Schubert, H. L., Stuckey, J. A., Fischer, M. W., Hume, D. M., Saper, M. A., and Dixon, J. E. (1992) Expression, purification, and physicochemical characterization of a recombinant Yersinia protein tyrosine phosphatase. *J. Biol. Chem.* 267, 23759–23766.
- Zalatan, J., Fenn, T., and Herschlag, D. (2008) Comparative enzymology in the alkaline phosphatase superfamily to determine the catalytic role of an active-site metal ion. *J. Mol. Biol.* 384, 1174–1189.
- O'Brien, P. J., Lassila, J. K., Fenn, T. D., Zalatan, J. G., and Herschlag, D. (2008) Arginine coordination in enzymatic phosphoryl transfer: Evaluation of the effect of Arg166 mutations in *Escherichia coli* alkaline phosphatase. *Biochemistry* 47, 7663–7672.
- Zalatan, J., and Herschlag, D. (2006) Alkaline phosphatase mono- and diesterase reactions: Comparative transition state analysis. *J. Am. Chem. Soc.* 128, 1293–1303.
- Wu, L., and Zhang, Z. Y. (1996) Probing the function of Asp128 in the lower molecular weight protein-tyrosine phosphatase-catalyzed reaction. A pre-steady-state and steady-state kinetic investigation. *Biochemistry* 35, 5426–5434.
- O'Brien, P. J., and Herschlag, D. (2001) Functional interrelationships in the alkaline phosphatase superfamily: phosphodiesterase activity of *Escherichia coli* alkaline phosphatase. *Biochemistry* 40, 5691–5699.
- Zhang, Z. Y. (1998) Protein-Tyrosine phosphatases: Biological function, structural characteristics, and mechanism of catalysis. *Crit. Rev. Biochem. Mol. Biol.* 33, 1–52.
- Zhang, Z. Y., and Dixon, J. E. (1994) Protein tyrosine phosphatases: Mechanism of catalysis and substrate specificity. *Adv. Enzymol. Relat. Areas Mol. Biol.* 68, 1–36.



- (24) Barford, D., Das, A. K., and Egloff, M. P. (1998) The structure and mechanism of protein phosphatases: Insights into catalysis and regulation. *Annu. Rev. Biophys. Biomol. Struct.* 27, 133–164.
- (25) Zhang, Z. Y., Wang, Y. A., and Dixon, J. E. (1994) Dissecting the catalytic mechanism of protein-tyrosine phosphatases. *Proc. Natl. Acad. Sci. U.S.A.* 91, 1624–1627.
- (26) Fischer, E. H., Charbonneau, H., and Tonks, N. K. (1991) Protein tyrosine phosphatases - a diverse family of intracellular and transmembrane enzymes. *Science* 253, 401–406.
- (27) Labow, B. I., Herschlag, D., and Jencks, W. P. (1993) Catalysis of the hydrolysis of phosphorylated pyridines by alkaline phosphatase has little or no dependence on the  $pK_a$  of the leaving group. *Biochemistry* 32, 8737–8741.
- (28) Hengge, A. C., Edens, W. A., and Elsing, H. (1994) Transition-state structures for phosphoryl-transfer reactions of p-nitrophenyl phosphate. *J. Am. Chem. Soc.* 116, 5045–5049.
- (29) Simopoulos, T. T., and Jencks, W. P. (1994) Alkaline phosphatase is an almost perfect enzyme. *Biochemistry* 33, 10375–10380.
- (30) O'Brien, P. J., and Herschlag, D. (2002) Alkaline phosphatase revisited: Hydrolysis of alkyl phosphates. *Biochemistry* 41, 3207–3225.
- (31) Kirby, A., and Jencks, W. (1965) The reactivity of nucleophilic reagents toward the p-nitrophenyl phosphate dianion. *J. Am. Chem. Soc.* 87, 3209–3216.
- (32) Kirby, A., and Varvoglis, A. (1967) The reactivity of phosphate esters. Monoester hydrolysis. *J. Am. Chem. Soc.* 89, 415–423.
- (33) Thatcher, G. R. J., and Kluger, R. (1989) Mechanism and catalysis of nucleophilic substitution in phosphate esters. *Adv. Phys. Org. Chem.* 25, 99–265.
- (34) Hengge, A. (2005) Mechanistic studies on enzyme-catalyzed phosphoryl transfer. *Adv. Phys. Org. Chem.* 40, 49–108.
- (35) Benkovic, S. J., and Benkovic, P. A. (1966) Studies on sulfate esters. I. Nucleophilic reactions of amines with p-nitrophenyl sulfate. *J. Am. Chem. Soc.* 88, 5504–5511.
- (36) Fendler, E. J., and Fendler, J. H. (1968) Hydrolysis of nitrophenyl and dinitrophenyl sulfate esters. *J. Org. Chem.* 33, 3852–3859.
- (37) Hopkins, A., Day, R. A., and Williams, A. (1983) Sulfate group transfer between nitrogen and oxygen: Evidence consistent with an open “exploded” transition state. *J. Am. Chem. Soc.* 105, 6062–6070.
- (38) Bourne, N., Hopkins, A., and Williams, A. (1985) Single transition state for sulfonyl group ( $-SO_3^-$ ) transfer between pyridine nucleophiles. *J. Am. Chem. Soc.* 107, 4327–4331.
- (39) Lassila, J. K., Zalatan, J. G., and Herschlag, D. (2011) Biological phosphoryl transfer reactions: Understanding mechanism and catalysis. *Annu. Rev. Biochem.* 80, 669–702.
- (40) Catrina, I., O'Brien, P. J., Purcell, J., Nikolic-Hughes, I., Zalatan, J. G., Hengge, A. C., and Herschlag, D. (2007) Probing the origin of the compromised catalysis of *E. coli* alkaline phosphatase in its promiscuous sulfatase reaction. *J. Am. Chem. Soc.* 129, 5760–5765.
- (41) Zalatan, J. G., Catrina, I., Mitchell, R., Grzyska, P. K., O'Brien, P. J., Herschlag, D., and Hengge, A. C. (2007) Kinetic isotope effects for alkaline phosphatase reactions: Implications for the role of active-site metal ions in catalysis. *J. Am. Chem. Soc.* 129, 9789–9798.
- (42) Nikolic-Hughes, I., Rees, D. C., and Herschlag, D. (2004) Do electrostatic interactions with positively charged active site groups tighten the transition state for enzymatic phosphoryl transfer? *J. Am. Chem. Soc.* 126, 11814–11819.
- (43) Hengge, A. C., Edens, W. A., and Elsing, H. (1994) Transition-state structures for phosphoryl-transfer reactions of p-nitrophenyl phosphate. *J. Am. Chem. Soc.* 116, 5045–5049.
- (44) Hoff, R. H., Larsen, P., and Hengge, A. C. (2001) Isotope effects and medium effects on sulfonyl transfer reactions. *J. Am. Chem. Soc.* 123, 9338–9344.
- (45) Sigala, P., Kraut, D., Caaveiro, J., Pybus, B., Ruben, E., Ringe, D., Petsko, G., and Herschlag, D. (2008) Testing geometrical discrimination within an enzyme active site: Constrained hydrogen bonding in the ketosteroid isomerase oxyanion hole. *J. Am. Chem. Soc.* 130, 13696–13708.
- (46) Fuhrmann, C. N., Kelch, B. A., Ota, N., and Agard, D. A. (2004) The 0.83 Å resolution crystal structure of alpha-lytic protease reveals the detailed structure of the active site and identifies a source of conformational strain. *J. Mol. Biol.* 338, 999–1013.
- (47) Elias, M., Wellner, A., Goldin-Azulay, K., Chabriere, E., Vorholt, J., Erb, T., and Tawfik, D. S. (2012) The molecular basis of phosphate discrimination in arsenate-rich environments. *Nature* 491, 134–137.
- (48) Abell, K., and Kirby, A. (1986) Acceleration of P-O cleavage reactions of phosphate monoester dianions in dipolar aprotic solvents. *Tetrahedron Lett.* 27, 1085–1088.
- (49) Montserat, J., Chen, L., Lawrence, D. S., and Zhang, Z. Y. (1996) Potent low molecular weight substrates for protein-tyrosine phosphatase. *J. Biol. Chem.* 271, 7868–7872.
- (50) McDonald, W. S., and Cruickshank, D. W. (1971) Crystal structure of dipotassium ethyl phosphate tetrahydrate  $K_2(C_2H_5)_2PO_4 \cdot 4H_2O$ : A problem in pseudo-symmetry. *Acta Crystallogr. B* 27, 1315–1319.
- (51) Jarvis, J. A. J. (1953) Crystal structure of potassium ethyl sulphate. *Acta Crystallogr.* 6, 327–330.
- (52) Truter, M. R. (1958) A detailed refinement of the crystal structure of potassium ethyl sulphate. *Acta Crystallogr.* 11, 680–685.
- (53) Sali, A., and Blundell, T. L. (1993) Comparative protein modeling by satisfaction of spatial restraints. *J. Mol. Biol.* 234, 779–815.
- (54) DeLano, W. (2007) MacPyMOL: A PyMOL-based molecular graphics application for MacOS X, DeLano Scientific LLC, Palo Alto, CA.
- (55) Baker, N. A., Sept, D., Joseph, S., Holst, M. J., and McCammon, J. A. (2001) Electrostatics of nanosystems: Application to microtubules and the ribosome. *Proc. Natl. Acad. Sci. U.S.A.* 98, 10037–10041.
- (56) Zhang, M., Zhou, M., Van Etten, R. L., and Stauffacher, C. V. (1997) Crystal structure of bovine low molecular weight phosphotyrosyl phosphatase complexed with the transition state analog vanadate. *Biochemistry* 36, 15–23.
- (57) Bobyr, E., Lassila, J., Wiersma-Koch, H., Fenn, T., Lee, J., Nikolic-Hughes, I., Hodgson, K., Rees, D., Hedman, B., and Herschlag, D. (2012) High-resolution analysis of Zn<sup>2+</sup> coordination in the alkaline phosphatase superfamily by EXAFS and x-ray crystallography. *J. Mol. Biol.* 415, 102–117.